JOURNAL OF Materials CHEMISTRY

Electrochemically assisted deposition of titanium dioxide on aluminium cathodes

Ana M. Peiró,[a] Enric Brillas,[b] José Peral,[a] Xavier Domènech[a] and José A. Ayllón*[a]

[a]*Unitat de Química-Física, Departament de Química, Universitat Autònoma de Barcelona, 08193 Bellaterra, Spain*
[b]*Laboratori de Ciència i Tecnologia Electroquímica de Materials (LCTEM), Departament de Química Física, Facultat de Química, Universitat de Barcelona, Martí i Franquès 1, 08028 Barcelona, Spain*

Received 23rd April 2002, Accepted 6th June 2002
First published as an Advance Article on the web 25th July 2002

Adherent, uniform, and porous TiO_2 films have been obtained at ambient temperature by a novel electrochemical process involving the simultaneous cathodic electrodeposition of a Ti(IV)–peroxo complex and electrophoretic deposition of nanocrystalline TiO_2 particles on an Al cathode. Electrodepositions were performed using an electrolytic suspension containing a water-soluble titanium complex stabilized with a peroxo ligand and a commercial nanocrystalline TiO_2 powder (Degussa P25), and by applying a constant cell voltage between 2.0 and 4.5 V. The reduction process favours the decomposition of the soluble titanium complex to yield an amorphous TiO_2 precipitate on the cathode. This amorphous precipitate also acts as a binder to the nanocrystalline TiO_2 particles. The whole assembly shows photocatalytic activity for the degradation of salicylic acid without the need of thermal post-treatment.

1. Introduction

In recent years, there has been great interest in the preparation of TiO_2 films for their application in different technological fields, such as photocatalysis,[1–3] dye sensitized solar cells,[4–6] antireflective coatings,[7,8] and electrochromic devices.[9,10] A large number of techniques such as sol–gel,[11] CVD,[12] sputtering,[13] self-assembled monolayers,[14,15] liquid phase deposition,[16] atomic layer deposition,[17,18] and Langmuir–Blodgett[19] have been utilized for the fabrication of TiO_2 films. The development of new low-cost processes, which are of environmental interest, for the deposition of such films is of considerable interest. Electrochemical techniques using aqueous solutions provide an attractive approach to meeting these needs.

Some recent studies have shown that cathodic electrodeposition of TiO_2 films holds great promise for various applications.[20,21] This method is usually based on the electrochemical production of OH^- from the cathodic reduction of water or dissolved oxygen that promotes the precipitation on the cathodic substrate deposits of oxides and/or hydroxides of metallic ions or complexes contained in the electrolytic medium. However, although this process is performed at low temperatures, a post-annealing treatment is usually required to crystallize the amorphous deposit initially obtained. This technique has been successfully used to produce films of several oxides such as ZrO_2,[22] WO_3,[23] $ZrTiO_2$,[22] Nb_2O_5,[20] and ZnO,[21–24] as well as several composites, *e.g.* RuO_2–TiO_2 and Al_2O_3–TiO_2.[20] Several authors[9,20,25] have also reported the cathodic electrodeposition of TiO_2 films from soluble peroxo complexes in aqueous or aqueous alcohol solutions. The process is carried out in two-steps: in the first one, the soluble peroxo complexes are transformed by an electrogenerated base into insoluble species ($Ti(O_2)O_x{\cdot}H_2O$) which precipitate on the cathode, while in the second step this solid titania precursor, still containing the peroxo ligand and with an amorphous nature, is thermally decomposed. Crystallization to anatase is attained at 773 K.

Electrophoretic deposition is another electrochemical approach to the fabrication of ceramic films. This technique has allowed the preparation of films of several simple oxides such as alumina, zirconia,[26,27] TiO_2,[27–29] and composites (*e.g.* alumina–zirconia micro-laminate).[30,31] Although crystalline ceramic particles were employed in all the precursor suspensions, an annealing post-treatment at elevated temperature was necessary to sinterize the particles and produce well adhered dense films (*i.e.*, 573 K is the minimum temperature required to produce stable TiO_2 films on stainless steel[28]).

The aim of the present work is to combine both processes, cathodic electrodeposition and electrophoretic deposition, with the goal of obtaining photoactive TiO_2 films without the need of a thermal post-treatment. An aqueous electrolytic suspension for this novel electrochemical method has been chosen for environmental interest. The idea is that the electrodeposit formed from the soluble Ti(IV)–peroxo complex should act as a matrix that captures the nanocrystalline TiO_2 particles present in the electrolytic suspension. A high number of these nanoparticles should not be completely occluded by the matrix, their surface thus being accessible to yield photocatalytic processes. According to previous studies,[20] this matrix is expected to be composed of an insoluble polymeric titanium–peroxo complex. However, under the experimental conditions tested, the peroxo ligand decomposes, probably being cathodically reduced, and the matrix is thus transformed into conducting amorphous TiO_2. The photocatalytic activity of the deposited films has been tested in the degradation of an organic model compound such as salicylic acid (SA) in aqueous medium.

2. Experimental

2.1. Reagents

Titanium dioxide P25 (TiO_2 P25, 80% anatase, 20% rutile) was kindly supplied by Degussa. Tetraisopropyl orthotitanate (TIP) was from Fluka; nitric acid (HNO_3, 52.5%), absolute ethanol (EtOH) and concentrated hydrogen peroxide (H_2O_2, 30 wt% in H_2O) from Panreac, and salicylic acid from Merck. These chemicals were used without further purification. All solutions were prepared with high purity water produced by a Millipore Milli-Q system, with a conductivity lower than $6 \times 10^{-8}\,\Omega^{-1}\,cm^{-1}$ at 25 °C.

2.2. Preparation of the suspension for electrodeposition

Several procedures were attempted to prepare a stable electrolytic suspension, until an effective method was achieved: 0.375 g TiO_2 P25 (4.70 mmol) were ultrasonically dispersed in 25 mL of H_2O for 2 min and 360 μL of HNO_3 (4.71 mmol) were added afterwards. Then, 209 μL TIP (0.680 mmol) were dissolved in a mixture of 25 mL of EtOH and 70 μL of concentrated H_2O_2 (0.680 mmol). The solution of TIP was added dropwise to the suspension of TiO_2 P25 and the resulting suspension was homogenized by sonication for 10 min. The electrolytic medium thus obtained has a pH = 1.5, being stable at 298 K for more than 10 hours without separation of the TiO_2 powder.

2.3. Electrolytic cell and electrode cleaning

All electrodepositions were carried out in an open, one-compartment, cylindrical Pyrex cell of 120 cm^3 capacity having an external water jacket for temperature control. The cell contained the cathode centred between two parallel and equidistant anodes, with a gap of 1.4 cm. The dimensions of each electrode were 28 mm in length × 20 mm in width. Two nets (10 mm × 5 mm × 1 mm of mesh) of platinized titanium (with 2 μm of Pt thickness) supplied by Inagasa were used as Pt anodes. The cathode was an aluminium foil of 1 mm thickness, always being placed into the electrolytic suspension with an immersed surface area of 5.6 cm^2 each side. Before the electrodeposition process, both anodes were cleaned in a hot NaOH (0.25 M) solution for several minutes, and rinsed several times with bidistilled water and finally, with Milli-Q water. The cathode was polished with a sand bath, and consecutively sonicated with bidistilled water, ethanol, acetone and Milli-Q water. All electrolytic experiments were conducted in the potentiostatic mode using an Amel 2053 potentiostat-galvanostat. A constant cell voltage was applied ranging from 2.0 to 4.5 V. The electrolytic suspension was not stirred and its temperature was maintained at 298 K. After each electrodeposition trial, the coated aluminium foil was removed from the cell, rinsed several times with Milli-Q water to eliminate the residual components of the suspension and dried in an open atmosphere up to a constant weight. The weight of electrodeposited TiO_2 was then determined as the mass difference between the coated and uncoated cathode.

2.4. Characterization techniques

The surface morphology and thickness of the films were studied by scanning electron microscopy (SEM) with a Hitachi S-570 microscope. Samples were gold-covered for all SEM measurements. For thickness studies, samples were mounted onto a holder with an inclination of 45 degrees with respect to the electron beam. The crystalline phase of the films was analyzed by grazing angle X-ray diffraction (XRD) with a Siemens D-3400 diffractometer using Cu-K_α radiation ($\lambda = 0.154056$ Å) at 40 kV and 30 mA. The diffraction spectra were recorded at an incidence angle of 1.8 degrees over the degree range $15 < 2\theta < 65$.

2.5. Photocatalytic activity measurements

The degradation of SA under UV illumination was used as a test of the photocatalytic activity of the films. Experiments were carried out with films obtained at a cell voltage of 3.50 V after an electrodeposition time of 90 min. The TiO_2 film was placed in a 100 mL aqueous solution of 0.25 mmol L^{-1} SA filling a thermostated cylindrical Pyrex cell, in which the temperature was kept at 298 K. The solution was maintained under stirring with a magnetic bar throughout the experiment, and air was bubbled through it. A 125 W Philips HPK medium-pressure mercury vapour lamp was used as light source. The TiO_2-covered aluminium foil was placed parallel to the light direction in the middle of the lamp's beam so that both faces were illuminated. The SA concentration was followed by measuring the absorbance of aliquots with a Philips PU 8620 UV/VIS/NIR spectrophotometer at a wavelength of 296 nm (the maximum of the absorption peak of SA). Quartz cuvettes of 1 cm optical path length were used.

3. Results and discussion

3.1. Preparation and composition of TiO_2 films

The electrolytic suspension used for electrodeposition contains nanocrystalline TiO_2 particles at pH = 1.5. This pH value is well below the pH of zero charge of TiO_2 (pH = 6.2) and thus, the particles are expected to be positively charged by adsorbed protons. On the other hand, when TIP is dissolved in absolute EtOH and H_2O_2 is added, a yellow solution is obtained due to the formation of peroxotitanium complexes, which prevent the condensation of Ti cations. In the electrolytic suspension of pH 1.5, these complexes are also positively charged and their main components are dinuclear species.[30] The existence of positive charges also impedes the adsorption of such titanium soluble species on the TiO_2 electrodeposits.

Electrolyses were carried out by applying a constant cell voltage higher than 2.0 V between the electrodes, trying to induce two parallel electrodeposition processes (cathodic and electrophoretic) on the Al cathode. At these high cell voltages, both processes also compete with the fast electrogeneration of OH^- from the reduction of dissolved oxygen, and/or the depletion of protons by their reduction to hydrogen gas. Thus, when the positively charged peroxotitanium complex reaches the vicinity of the cathode, where the pH is basic due to the presence of electrogenerated OH^- ions, it reacts with the precipitation of an insoluble peroxotitanium hydrate, $TiO_3(H_2O)_x$ ($1 < x < 2$).[20,22,32] In addition, the positively charged TiO_2 nanoparticles move electrophoretically toward the cathode, being codeposited with the above mentioned peroxotitanium hydrate. Electrodeposited TiO_2 films thus obtained were white, as expected when no peroxo species are present, at least not in any significant proportion. This point was confirmed by the high stability of the films when treated with strong acidic solution (HNO_3 or HCl) at room temperature. It can then be inferred that during the electrolytic process, the insoluble $TiO_3(H_2O)_x$ decomposes, probably by cathodic reduction, and for this reason it is not present in the final TiO_2 electrodeposit. It is noteworthy that the yellow colour of the suspension faded away as the electrodeposition process took place, while the pH of the solution remained practically constant throughout the electrolysis (near 1.5), indicating that all the soluble peroxo species are consumed in the process.

The composition of the deposits was characterized using XRD. Fig. 1 shows the XRD patterns of a TiO_2 film electrodeposited at a constant cell voltage of 3.50 V for 30 min. According to the JCPDS reference data, the main diffraction lines were identified as those corresponding to TiO_2 anatase (A), TiO_2 rutile (R) and aluminium (Al); very small peaks due to Al_2O_3 were also observed. Anatase and rutile phases are present in the films in the same ratio as in TiO_2 P25, confirming that the nanocrystalline TiO_2 powder has been incorporated into the films. These results rule out the formation of crystalline TiO_2 from the possible cathodic reduction of insoluble $TiO_3(H_2O)_x$. Due to the low temperature of the process, the titania formed in the reduction of the soluble peroxotitanium precursor (which accounts for 14% of the titanium contained in the electrolytic suspension) should be amorphous, and therefore, will not exhibit any diffraction peak.

Efforts were then devoted to show the presence of amorphous titania in the films produced by the proposed

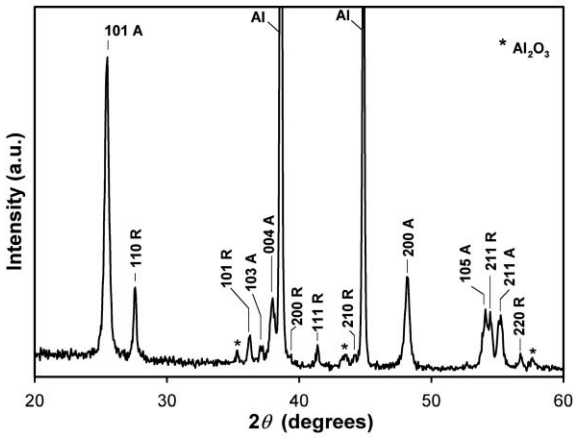

Fig. 1 Grazing incidence X-ray diffractogram corresponding to a TiO_2 film electrodeposited onto an aluminium substrate. The main diffraction peaks correspond to anatase (A), rutile (R), and aluminium substrate (Al). Applied cell voltage 3.50 V. Electrodeposition time 30 min. Temperature 298 K.

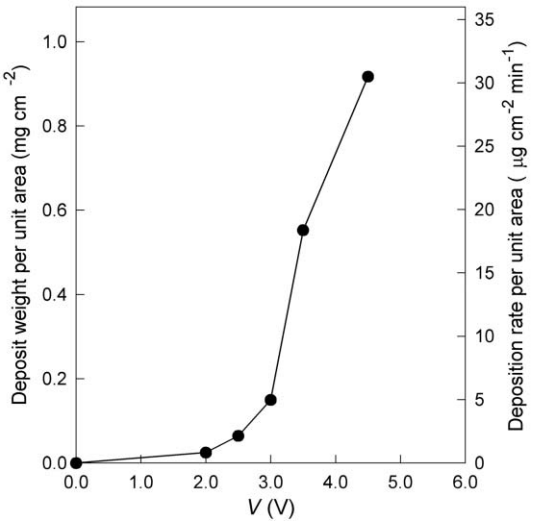

Fig. 2 Variation of the weight of electrodeposited TiO_2 or its electrodeposition rate per unit area with applied cell voltage over 30 min. Temperature 298 K.

electrochemical method. Initial confirmation was made by treating the electrodeposits with a solution containing H_2O_2 and strong acid. In these treatments, yellow solutions were obtained leading to a partial detachment of films, which can be ascribed to the partial solubilization of amorphous titania contained in them. In addition, several electrolyses were also performed without the soluble peroxotitanium precursor in the electrolytic bath, but no films grew on the cathode surface. This behaviour allows us to establish that the amorphous titania produced from the insoluble $TiO_3(H_2O)_x$ acts as a binder of the codeposited nanocrystalline TiO_2 particles.

3.2. Electrodeposition behavior

Different electrolytic conditions were tested in an attempt to obtain TiO_2 electrodeposits. The use of a constant current led to a progressive increase in cell voltage producing deposits of very low adherence. The potentiostatic method was preferred because adherent, uniform, and white deposits grew by applying a constant cell voltage ranging from 2.0 to 4.5 V for times of up to 90 min. However, lower cell voltages did not yield films, probably because of the low electrogeneration rate of OH^- that prevents cathodic electrodeposition of the soluble titanium complex, whereas cell voltages higher than 4.5 V caused a fast stripping of deposits.

Fig. 2 shows a non-linear behaviour of the weight of deposited material at the cathode per unit area, or the rate of electrodeposition per unit area, with increasing voltage for a fixed electrodeposition time of 30 min. As can be seen, the electrodeposition rate is moderately low below 3.0 V, but rapidly increases to *ca.* 30 μg cm^{-2} min^{-1} at 4.50 V. Fig. 3 presents the change of deposit weight per unit area *vs.* the electrodeposition time for a constant cell voltage of 3.50 V. Faradaic behaviour can be observed until 60 min, for which an average electrodeposition rate of *ca.* 17 μg cm^{-2} min^{-1} is obtained. However, at 90 min, the deposit weight is lower than expected, while longer times promote a partial film stripping.

The data in Figs. 2 and 3 allow us to conclude that the amount of electrodeposited TiO_2 can be controlled either by adjusting the applied cell voltage at a fixed electrodeposition time or by varying such time at a given cell voltage, always limiting the cell voltage to between 2.0 and 4.5 V and the electrodeposition time to 90 min. Under these conditions, a relatively high cathodic current density (j_{cat}) is always found. This can be observed in Fig. 4, where the time dependence of j_{cat} for a cell voltage of 3.50 V is depicted. Similar j_{cat}–t curves were obtained for other experiments performed under the

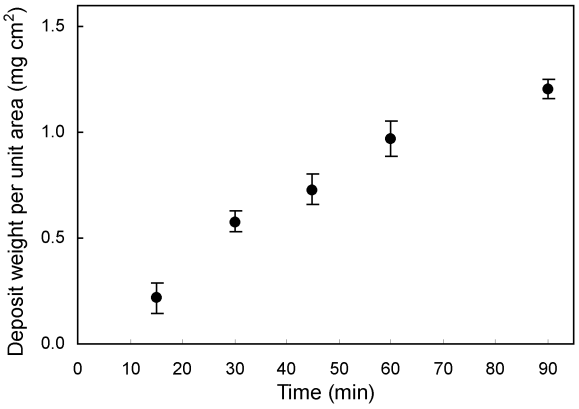

Fig. 3 Dependence of the weight of electrodeposited TiO_2 on electrodeposition time for a constant cell voltage of 3.50 V. Temperature 298 K.

conditions shown in Fig. 3. In all cases, the initial cathodic current density drops rapidly reaching a value of *ca.* 5.2 mA cm^{-2} after the first minute, when a thin film already covers the immersed cathode surface. The subsequent slight, but gradual, decay of j_{cat} with time can be ascribed to the increasing electrical resistance of the thickening coating.

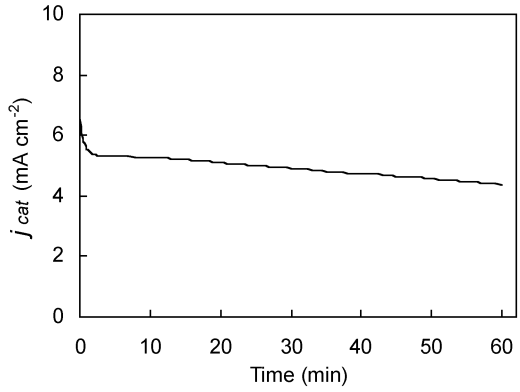

Fig. 4 Cathodic current density *vs.* electrodeposition time on applying a constant cell voltage of 3.50 V. Temperature 298 K.

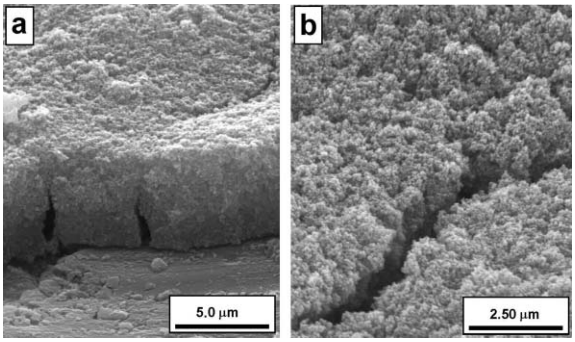

Fig. 5 SEM images taken at 45 degrees for a TiO_2 film electrodeposited for 90 min on Al: (a) cross-section of a step; (b) detail showing the porous texture of the film. Applied cell voltage 3.50 V. Temperature 298 K.

3.3. Thickness and morphology of TiO_2 electrodeposits

The thickness of the films was measured using both SEM and weight methods. As an example, two SEM cross-sections of the TiO_2 electrodeposits obtained after different times are depicted in Fig. 5. Although no regular films can be observed, SEM measurements allowed us to measure an electrodeposition rate of approximately 0.15 μm min^{-1} under the conditions given in Fig. 3 for a cell voltage of 3.50 V. On the other hand, the average thickness of these deposits was also calculated from its weight, once the area of the covered substrate was known, and by assuming that the films are compact (weight method). The density of electrodeposited TiO_2 required for this calculation was assumed to be the same as that of TiO_2 P25 supplied by Degussa,[33] *i.e.* 3.7 g cm^{-3}, because of the similar structure of both materials, as above pointed out. The thickness of the films were estimated by this method to be between 2 and 4.5 times lower than those experimentally obtained by SEM measurements. This difference clearly indicates that the films are porous. In fact, the high porosity of the films can be readily observed in the SEM image of Fig. 5(b).

The surface morphology of TiO_2 electrodeposited films on Al was also studied by SEM. As it is shown in Figs. 6(b)–6(e), all deposits obtained with a cell voltage of 3.50 V exhibit significant cracking, which may be related to the drying process or be induced by the Al substrate morphology (see Fig. 6(a)). The Al substrate presents a rough surface that can affect not only the morphology of the deposit but its adhesion, as well. To clarify this point, supplementary electrodepositions were performed under the same conditions using Al cathodes, polished using a combination of a sand paper and diamond grit polishing paste of 6 and 1 μm, respectively. For these experiments, less TiO_2 was electrodeposited than experiments performed with rougher Al surfaces, but similar cracking was observed in both cases. These results allow us to conclude that cracking occurs during the drying process.

3.4. Photocatalytic activity of electrodeposited TiO_2 films

The photocatalytic activity of the electrodeposited TiO_2 films was studied by testing their ability to degrade a 100 mL solution of 0.25 mmol L^{-1} salicylic acid. This acid has been chosen as a model compound to test the activity of TiO_2 in a large number of papers,[34–38] not only because it is a common pollutant in industrial waste waters (paper milling, cosmetic industries, landfill leachate),[39] but also because its molecular structure is similar to many other toxic compounds. Comparative trials were carried out using the SA solution with and without an Al substrate coated with a TiO_2 film deposited at 3.50 V for 90 min. In each case, treatment in the dark for 120 min was performed initially to evaluate possible adsorption phenomena or instability of the system, followed by exposure to UV light for 150 min. The relative concentration of SA,

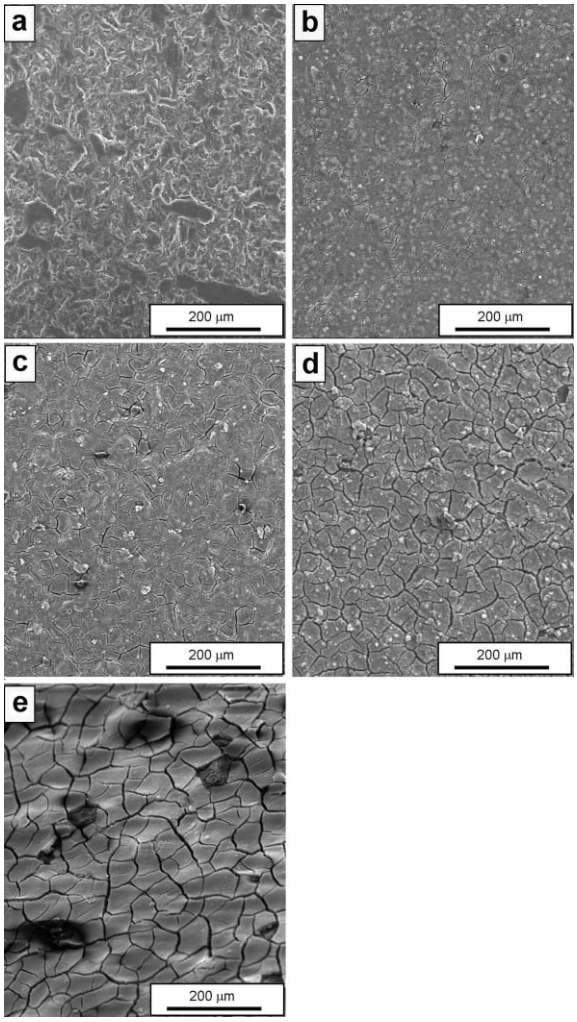

Fig. 6 SEM micrographs showing the surface morphology of (a) Al substrate and of TiO_2 films electrodeposited on Al cathodes after different periods of time: (b) 30, (c) 45, (d) 60, and (e) 90 min. Applied cell voltage 3.50 V. Temperature 298 K.

determined as the ratio between the absorbance at time t and the initial absorbance, both at 296 nm, is depicted in Fig. 7. Reproducible results were obtained for different films prepared and used under the same experimental conditions. From the data in Fig. 7, it can be inferred that there is no loss of the organic compound by volatilization or air stripping, since in the dark and without TiO_2, no change in the SA concentration

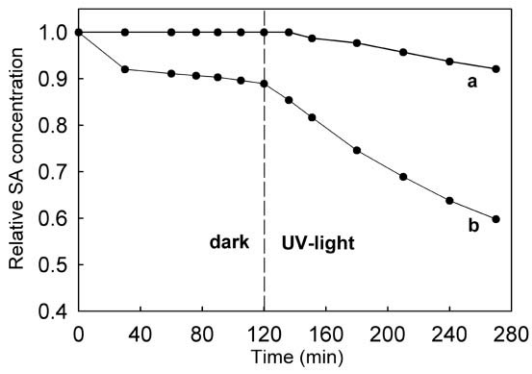

Fig. 7 Time course of the relative concentration of SA in aqueous solution: (a) in the dark without TiO_2, followed by UV illumination; and (b) in the dark with a TiO_2 film, followed by UV illumination. Experimental conditions: $[SA]_0$ = 0.25 mmol L^{-1}, pH_0 = 3.0, air bubbling, irradiation with a 125 W medium pressure Hg vapour lamp, and temperature 298 K. The TiO_2 electrodeposit was prepared at a constant cell voltage of 3.50 V for 90 min.

was noticed. In the dark and in the presence of a TiO_2 film, a fast decrease in the concentration of salicylic acid, stabilized to *ca.* 10%, takes place as a consequence of its adsorption on the catalyst surface. As can be seen in Fig. 7(b), illumination of the solution in the presence of a TiO_2 film leads to a significant reduction in the SA concentration: about 30% in 150 min. The percentage of SA degraded by direct photolysis in the same time (see Fig. 7(a)) is less than 5%, a negligible value compared to the removal observed with a TiO_2 film. Considering that amorphous titania is not photoactive,[40] the photoactivity detected for the electrodeposited films should be ascribed to the existence of nanocrystalline TiO_2 at their surface. This fact indicates that during electrodeposition TiO_2 particles are not completely occluded by the amorphous TiO_2 binder.

Conclusions

It has been demonstrated that adherent, uniform, and porous TiO_2 films can be electrodeposited on aluminium at ambient temperature with a novel electrochemical method that involves the simultaneous cathodic and electrophoretic deposition of two titania species present in a stable aqueous suspension. This process is possible using a constant cell voltage between 2.0 and 4.5 V, conditions under which OH^- is also electrogenerated in the vicinity of the cathode. Thus, electrophoretically deposited nanocrystalline TiO_2 particles can be immobilised onto the metal substrate by an amorphous TiO_2 matrix produced from the cathodic electrodeposition of a soluble peroxotitanium precursor. This last process involves the initial precipitation of a peroxotitanium hydrate by reaction of this precursor with electrogenerated OH^-, followed by its decomposition, probably by cathodic reduction, to the final conducting amorphous titania. The film thickness can be controlled either by the cell voltage applied and/or by its electrodeposition time up to 90 min. The films show photocatalytic activity without the need of thermal post-treatment, indicating that their nanocrystalline TiO_2 particles are not completely occluded by the amorphous titania matrix.

References

1 R. L. Pozzo, M. A. Baltanás and A. E. Cassano, *Catal. Today*, 1997, **39**, 219–231.
2 Y. Jiaguo, Z. Xiujian and X. Qingnan, *Mater. Chem. Phys.*, 2001, **69**, 25–29.
3 A. P. Xagas, E. Androulaki, A. Hiskia and P. Falaras, *Thin Solid Films*, 1999, **357**, 173–178.
4 Y. Li, J. Hagen, W. Schaffrath, P. Otschik and D. Haarer, *Sol. Energy Mater. Sol. Cells*, 1999, **56**, 167–174.
5 C. J. Barbé, F. Arendse, P. Comte, M. Jirousek, F. Lenzmann, V. Shklover and M. Grätzel, *J. Am. Ceram. Soc.*, 1997, **80**, 3157–3171.
6 G. Phani, G. Tulloch, D. Vittorio and I. Skryabin, *Renewable Energy*, 2001, **22**, 303–309.
7 G. San Vicente, A. Morales and M. T. Gutierrez, *Thin Solid Films*, 2001, **391**, 133–137.
8 L. M. Doeswijk, H. H. C. de Moor, D. H. A. Blank and H. Rogalla, *Appl. Phys. A: Solid Surf.*, 1999, **69 (Suppl)**, S409–S411.
9 C. Natarajan and G. J. Nogami, *J. Electrochem. Soc.*, 1996, **143**, 1547–1550.
10 S. K. Poznyak, V. V. Sviridov, A. I. Kulak and M. P. Samtsov, *J. Electroanal. Chem.*, 1992, **340**, 73–97.
11 Y. Zhu, L. Zhang, L. Wang, Y. Fu and L. Cao, *J. Mater. Chem*, **11**, 1864–68.
12 B.-C. Kang, S.-B. Lee and J.-H. Boo, *Surf. Coat. Technol.*, 2000, **131**, 88–92.
13 D. Mardare, M. Tasca, M. Delibas and G. I. Rusu, *Appl. Surf. Sci.*, 2000, **156**, 200–206.
14 Y. Masuda, T. Sugiyama, H. Lin, W. S. Seo and K. Koumoto, *Thin Solid Films*, 2001, **382**, 153–157.
15 H. Shin, R. J. Collins, M. R. De Guire, A. H. Heuer and C. N. Sukenik, *J. Mater. Res.*, 1995, **10**, 692–698.
16 H. Kishimoto, K. Takahama, N. Hashimoto, Y. Aoi and S. Deki, *J. Mater. Chem.*, 1998, **8**, 2019–2024.
17 M. Ritala, M. Leskela, L. Niinisto and P. Haussalo, *Chem. Mater.*, 1993, **5**, 1174–1781.
18 M. Ritala, M. Leskela, E. Nykaenen, P. Soininen and L. Niinisto, *Thin Solid Films*, 1993, **225**, 288–295.
19 J. Jin, L. S. Li, Y. Li, X. Chen, L. Jiang, Y. Y. Zhao and T.-T. Li, *Thin Solid Films*, 2000, **379**, 218–223.
20 I. Zhitomirsky, *J. Eur. Ceram. Soc.*, 1999, **19**, 2581–2587.
21 S. Peulon and D. J. Lincot, *J. Electrochem. Soc.*, 1998, **145**, 864–874.
22 I. Zhitomirsky and L. Gal-Or, *J. Eur. Ceram. Soc.*, 1996, **16**, 819–824.
23 E. A. Meulenkamp, *J. Electrochem. Soc.*, 1997, **144**, 1664–1671.
24 M. Izaki and T. Omi, *J. Electrochem. Soc.*, 1997, **144**, 1949–1952.
25 I. Zhitomirsky, *Nanostruct. Mater.*, 1997, **8**, 521–528.
26 T. Uchikoshi, K. Ozawa, B. D. Hatton and Y. Sakka, *J. Mater. Res.*, 2001, **16**, 321–324.
27 I. Koengeter, I. Wuehrl, U. Eisele, R. Drumm, S. Knoll R. Nonninger and H. Schmidt, *Ger. P.*, 2000, 19919818.
28 J. A. Byrne, B. R. Eggins, N. M. D. Brown, B. Mckinney and M. Rouse, *Appl. Catal. B: Environ.*, 1998, **17**, 25–36.
29 D. Matthews, A. Kay and M. Graetzel, *Aust. J. Chem.*, 1994, **47**, 1869–1877.
30 R. Fischer, E. Fischer, G. de Portu and E. Roncari, *J. Mater. Sci. Lett.*, 1995, **14**, 25–27.
31 P. S. Nicholson, P. Sarkar and X. Haung, *J. Mater. Sci.*, 1999, **28**, 6274–6278.
32 J. Mühlenbach, K. Müller and G. Schwarzenbach, *Inorg. Chem.*, 1970, **9**, 2381–2390.
33 M. Ettingler, *Degussa Technical Bulletin Pigments*, vol. 56, Degussa AG, Frankfurt, Germany, 1993.
34 A. E. Regazzoni, P. Mandelbaum, M. Matsuyoshi, S. Schiller, S. A. Bilmes and M. A. Blesa, *Langmuir*, 1998, **14**, 868–874.
35 V. Sukharev, A. Wold, Y.-M. Gao and K. Dwight, *J. Solid State Chem.*, 1999, **119**, 339–343.
36 G. Li Puma and P. L. Yue, *Chem. Eng. Sci.*, 1998, **53**, 3007–3021.
37 S. Tunesi and M. Anderson, *J. Phys. Chem.*, 1991, **95**, 3399–3405.
38 K. Katrochrilova, I. Hoskovcová, J. Jirkovsky, J. Klíma and J. Ludvik, *Electrochim. Acta*, 1995, **40**, 2603–2609.
39 A. Mills, C. E. Holland, R. H. Davies and D. J. Worsley, *Photochem. Photobiol. A.: Chem.*, 1994, **83**, 257–263.
40 B. Ohtani, Y. Ogawa and S.-i. Nishimoto, *J. Phys. Chem. B*, 1997, **101**, 3746–3752.